JOURNAL OF CATALYSIS 128, 137–147 (1991)

In Situ Electron Microscopy Investigation of the Behavior of Supported Cobalt Particles

S. G. OH AND R. T. K. BAKER

Chemical Engineering Department, Auburn University, Auburn, Alabama 36849

Received July 11, 1990; revised October 1, 1990

In situ electron microscopy studies have shown that cobalt particles supported on graphite exhibit some very unexpected reactivity patterns during gasification reactions. When the reaction was performed in the presence of oxygen the cobalt particles were observed to initially wet and spread along graphite edges and accelerate the removal of carbon atoms from these locations by the edge recession mode. This type of action persisted up to temperatures of around 880°C at which point particles reformed and the mode of action changed to that of channeling. Quantitative kinetic analysis of these events showed the existence of three distinct activity regions, which corresponded to the formation of three oxidation states of cobalt, CoO (475–640°C), Co_3O_4 (665–880°C), and Co (>880°C), as determined from *in situ* electron diffraction analysis. It was significant that postreaction electron diffraction examination failed to show the presence of the metallic phase in specimens which had been cooled to room temperature. When colbalt/graphite specimens were treated in hydrogen, initial attack took place by the edge recession mode and was replaced by a channeling action at 650°C which coincided with the formation of particles at edge sites. This form of attack continued up to temperatures in excess of 1000°C, and the catalyst particles did not appear to show any tendency to deactivate. The results obtained in this study are compared with those found for iron and nickel from previous investigations.

INTRODUCTION

The ferromagnetic metals, iron, cobalt, and nickel, are used as catalysts for a number of commercial processes which are frequently operated under conditions where carbon deposition becomes a major source of catalytic deactivation. While a considerable body of information exists on the ability of iron and nickel to promote the removal of carbon in both oxidizing and reducing environments there are fewer reports on the behavior of cobalt in these reactions.

Thomas and Walker (*1*) used *in situ* optical microscopy to follow the behavior of cobalt particles deposited on graphite when heated in the presence of various gases. They reported that in an oxygen environment cobalt particles catalyzed attack of graphite by the channeling mode, and this behavior persisted for as long as particles remained in the metallic state. However, after a short period of time they were converted to oxide and this transformation coincided with a loss in catalytic activity.

McKee (*2*) used a combination of thermogravimetric analysis and *in situ* optical microscopy to investigate the influence of a number of oxides, including cobalt oxide on the graphite–oxygen reaction. He concluded that the oxide, Co_3O_4, was the most likely catalytic species in the reaction and was responsible for creating channels across the graphite basal planes. From bulk measurements, Heintz and Parker (*3*) obtained a value of 49.4 kcal/mole for the activation energy of the cobalt-catalyzed decomposition of graphite when oxidized in air at 600 to 700°C.

Tomita and co-workers (*4–6*) examined the effects of several transition metals on the graphite–hydrogen reaction and demon-

0021-9517/91 $3.00

strated that the reactivity of cobalt for this reaction is significantly lower than that of nickel and the majority of the noble metals.

In the present investigation we have used *in situ* electron microscopy techniques to follow the action of individual catalyst particles on the graphite–oxygen and graphite–hydrogen reactions and to determine the kinetics of the various stages involved in the gasification reactions. In a complementary series of experiments a novel approach involving *in situ* electron diffraction was used to determine the changes in the chemical nature of the catalyst particles as a function of increasing temperature and in the presence of either oxygen or hydrogen. The results obtained for cobalt are compared with those reported previously for nickel (*7, 8*) and iron (*9*) when reacted under the same conditions.

EXPERIMENTAL

The experiments reported in this paper were all performed by *in situ* transmission electron microscopy. The quantitative kinetic studies were carried out in a JEM 120 electron microscope fitted with an AGI reaction cell. The resolution of this instrument when used in conjunction with a closed-circuit television system is 2.5 nm (*10*). Detailed information of the chemical state of the catalyst under reaction conditions was obtained from *in situ* diffraction analysis using a modified JEOL 200CX TEM/STEM electron microscope. This instrument is equipped with a custom-designed environmental cell, which accommodates a heating stage. With this technique we estimate that the point-to-point resolution achieved on the TV monitor is of the order of 0.4 nm under sufficiently stable conditions (*11*). To our knowledge this is the first time that it has been possible to analyze the chemical state of particles as they are reacting, and from the data presented here it will be seen that major differences are obtained under these conditions compared to a postreaction examination of a specimen which had been cooled to room temperature. The analysis of the diffraction data was carried out by a newly developed computer program in which all possible compounds were incorporated. This program takes into consideration all crystallographic parameters and restricting rules for each spectroscopic plane and generates theoretical *d*-spacing data which allows one to perform the simulations necessary to compare with the experimental values. In this operation a 2% error between theoretical and experimental values was allowed.

Two procedures were used to introduce cobalt onto transmission specimens of single crystal graphite. In the first method, spectrographically pure cobalt (99.99% pure) was deposited onto the graphite substrates by evaporation from a tungsten filament at a residual pressure of 10^{-6} Torr. The conditions were chosen so as to produce a film of metal at least one atom in average thickness. In the second approach, the metal was introduced as an atomized spray from 0.1% aqueous solution of cobalt nitrate. The reactant gases used in this work, oxygen and hydrogen, were obtained from Alphagaz Co. with stated purities of 99.999% and used without further purification.

RESULTS

(*a*) *Cobalt/Graphite–Oxygen*

When graphite specimens containing added cobalt were heated in 2.0 Torr oxygen, nucleation of small particles (2.5–5.0 nm diam.) started at 450°C. At 475°C those particles which had collected at edge and step sites were observed to undergo a rapid transformation, first to a wetting state and then finally "disappearing" due to a spreading action to form a thin film along these regions. After holding at this temperature for a short period of time, the coated graphite edges were observed to gasify by a recession mode and even though these edges were relatively straight they did not appear to exhibit any preferred orientation. Figure

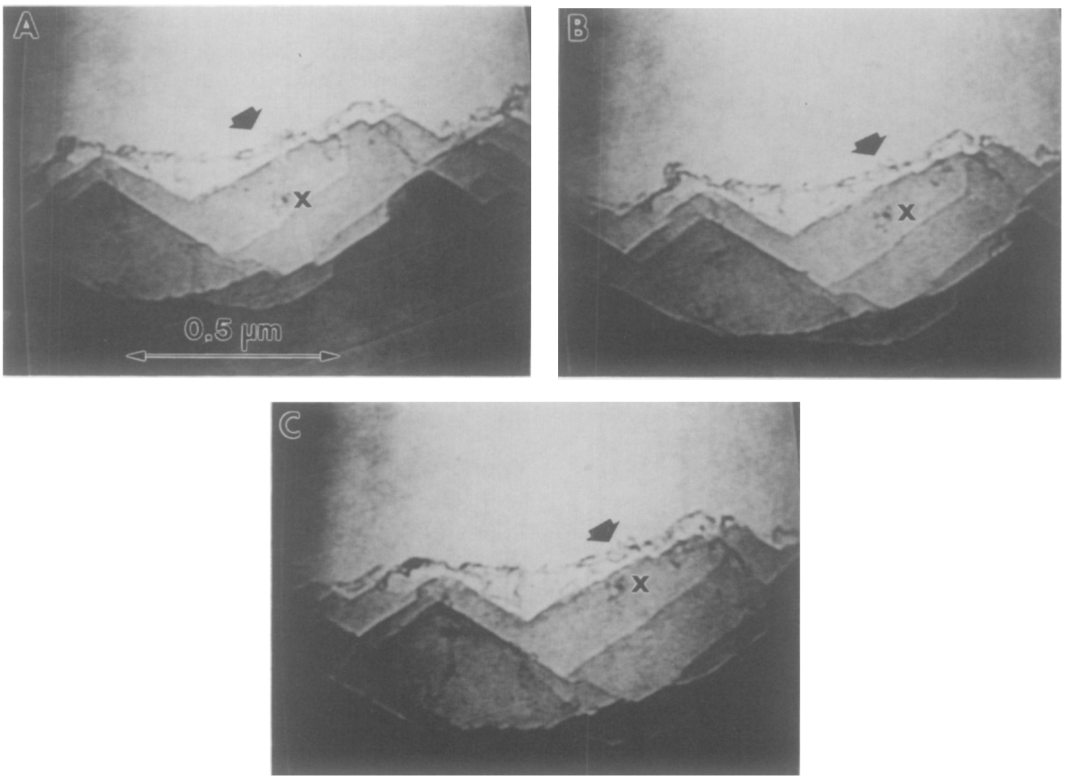

FIG. 1. (A–C) Sequence showing the cobalt-catalyzed attack of graphite in oxygen at 650°C by the edge recession mode. The direction of movement is indicated by the arrow and "x" is a reference point in the surface. Time interval between each frame is 10 sec.

1 is a sequence of photographs taken from the video display, showing the edge recession attack of graphite in oxygen at 650°C.

Edge recession remained the exclusive form of attack up to 880°C when the catalyst film ruptured leading to the reformation of particles at edges and steps. These particles then proceeded to catalyze the gasification reaction by creating channels across the graphite basal plane. It was evident that the channels did not follow any preferred orientation and that they maintained their initial width for considerable distances, indicating that at high temperatures there was a change in the wetting characteristics of the catalytic species on the graphite.

Detailed kinetic analysis of the dynamic events occurring during the reaction sequences of several experiments revealed that there were three separate activity regions; a low temperature edge recession mode from 475 to 640°C (designated 1), an intermediate temperature edge recession from 665 to 875°C (designated 2), and a high temperature channeling action from 875 to >1000°C. From Arrhenius plots of the variation of edge recession rates and channel propagation rates with temperature (Fig. 2), it has been possible to evaluate the apparent activation energies associated with the three activity regions; edge recession mode 1 = 42.4 ± 4 kcal/mole, edge recession mode 2 = 39.5 ± 4 kcal/mole, and channeling formation by 20-nm particles creating channels of similar depth = 30.1 ± 3 kcal/mole.

In a separate series of experiments the

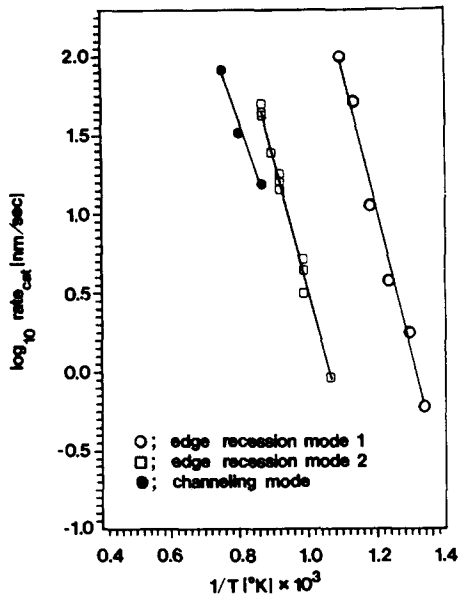

FIG. 2. Arrhenius plots for cobalt-catalyzed gasification of graphite in 2.0 Torr oxygen.

changes in chemical nature of the catalyst particles were followed by *in situ* electron diffraction as cobalt/graphite samples were heated in the presence of 0.5 Torr oxygen over the range 20 to 900°C. Some of the electron diffraction patterns obtained from these experiments are shown in Figs. 3A–3C, and the corresponding analytical data are presented in Tables 1 to 3, where the theoretical data are based on room temperature values. It is anticipated that changes in temperature will influence the values of the *d*-spacings for the various compounds, and in order to correct for this effect, the thermal linear expansion coefficients in the *a* and *c* directions were taken into account. This aspect is fully discussed in the Appendix. The presence of graphite offers a particular advantage since this material serves as an internal standard for calibration of all other patterns. From examination of the diffraction data it is evident that over the range 475 to 640°C, the predominant state of the catalyst is CoO, and as the temperature is raised above 665°C, an additional oxide, Co_3O_4, is formed, and at the highest temperatures, in excess of 880°C we see the emergence of the metallic phase.

It is of extreme importance to compare the electron diffraction pattern and analytical data (Fig. 3D and Table 4, respectively) of a cobalt/graphite specimen which had

TABLE 1

Electron Diffraction Analysis of Cobalt/Graphite during Reaction in Oxygen over the Range 475–655°C

Calculated *d*-spacings (nm)	*d*-Spacings for CoO (nm)
0.213	0.213
0.150	0.151

TABLE 2

Electron Diffraction Analysis of Cobalt/Graphite during Reaction in Oxygen over the Range 665–875°C

Calculated *d*-spacings (nm)	*d*-Spacings (nm)	
	Co_3O_4	CoO
0.287	0.286	
0.245		0.246
0.210		0.213
0.143	0.143	
0.123	0.123	

TABLE 3

Electron Diffraction Analysis of Cobalt/Graphite during Reaction in Oxygen at >880°C

Calculated *d*-spacings (nm)	*d*-Spacings (nm)		
	Co	Co_3O_4	CoO
0.286		0.286	
0.247			0.246
0.208	0.205		
0.162		0.165	
0.144		0.143	
0.126	0.125		

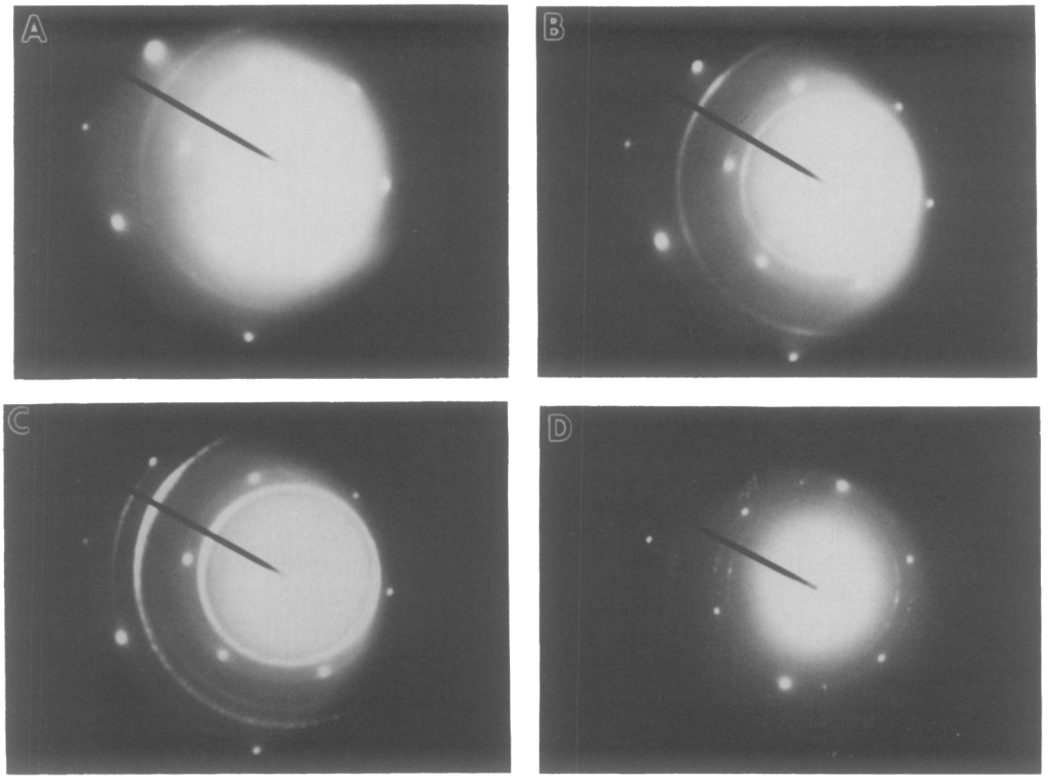

FIG. 3. Selected area electron diffraction patterns of cobalt/graphite specimens at various temperatures in 0.5 Torr oxygen. (A) 500°C, (B) 700°C, (C) 900°C, and (D) 25°C.

been cooled to room temperature after reaction in 0.5 Torr O_2 at 900°C with that obtained from the same specimen under reaction conditions. The patterns are quite different and the postreaction analysis shows no evidence for the presence of metallic cobalt. This aspect highlights the danger in drawing conclusions regarding the chemical state of a system based on measurements which have been performed on a specimen after cooling and removal from the reaction environment.

TABLE 4

Electron Diffraction Analysis of Cobalt/Graphite at Room Temperature after Reaction in Oxygen at 900°C

Calculated *d*-spacings (nm)	*d*-Spacings (nm)		
	Co	Co_3O_4	CoO
0.249			0.246
0.211			0.213
0.150			0.151
0.143		0.143	

(b) Cobalt/Graphite–Hydrogen

Treatment of the cobalt/graphite system in 1.0 Torr hydrogen resulted in the formation of particles at about 350°C. On continued heating, particles on the graphite basal plane increased in size, whereas those located on edge and step sites tended to disappear at 400°C as a consequence of a wetting and spreading action. This behavior preceded the onset of catalytic gasification, which occurred at 450°C by the edge recession mode. Initially the recession proceeded

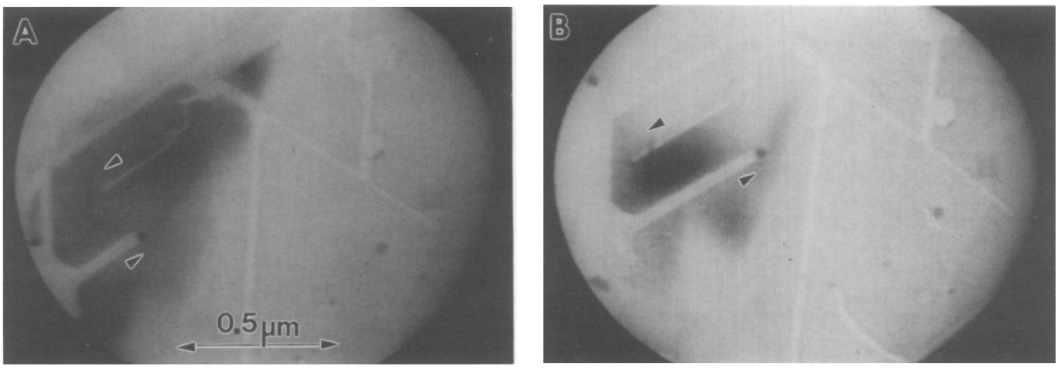

FIG. 4. (A,B) Development of channels across the graphite surface by cobalt particles at 800°C in 1.0 Torr hydrogen. Direction of channel movement is indicated by arrows. Time interval between frames is 15 sec.

in a random fashion; however, after a short time the edges required an angular profile in which sections were aligned in directions parallel to the $\langle 11\bar{2}0 \rangle$ crystallographic orientations of the graphite.

At 650°C there was a dramatic change in the mode of catalytic attack; edge recession came to a halt as particles reformed at these sites and then fresh particles proceeded to propagate channels across the graphite basal plane. The majority of channels were straight, being oriented predominantly parallel to the $\langle 11\bar{2}0 \rangle$ directions and occasionally altered course by executing turns through 60 and 120°, characteristics which are typical of catalytic hydrogenation of graphite (*8*). An example of this type of catalytic action is shown in Fig. 4. In contrast to nickel (*7, 8*), active cobalt particles preserved their initial size throughout the channel propagation process and maintained their activity at temperatures in excess of 1000°C. There was also evidence of particles moving across the graphite basal plane along relatively straight tracks and apparently not creating channels. This phenomenon could well have been due to the formation of monolayer channels as reported by other workers who used the gold decoration technique to reveal their existence (*12*). Such features would not be observed by the conventional transmission mode since there is only a minimal difference in the electron density between the channel and the surrounding unattacked region.

From analysis of the video recordings of these experiments it has been possible to obtain quantitative kinetic data on both the edge recession and the channeling processes, which are presented in the form of Arrhenius plots (Fig. 5). From the slopes of these lines, apparent activation energies of 16.3 ± 2 and 35.1 ± 3 kcal/mole were derived from the edge recession and channeling modes of attack, respectively. The latter plot is based on 25-nm particles cutting channels of similar depth.

DISCUSSION

(*a*) *Cobalt/Graphite–Oxygen*

From the present study it is evident that cobalt exhibits unique catalytic behavior in the graphite–oxygen reaction, possessing three distinct activity regimes. Direct determination of the changes in the chemical state of the catalyst by *in situ* electron diffraction shows that this pattern of activity can be correlated with the existence of three different chemical states: CoO at low temperatures, Co_3O_4 at intermediate temperatures, and Co metal at the highest temperatures. The formation of two oxidation states is also consistent with the thermogravimetric studies reported by McKee (*2*).

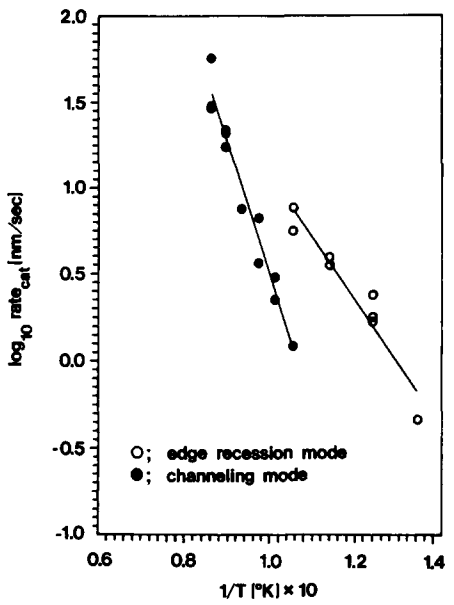

FIG. 5. Arrhenius plots for cobalt-catalyzed hydrogenation of graphite.

A further feature to emerge from the oxidation experiments is the manner by which the mode of catalytic attack changes as a function of reaction temperature. It is clear that when the catalytic specie is in an oxide state a strong interaction is established with the oxygenated graphite edge and step sites and the subsequent attack occurs by edge recession. On the other hand, when conditions are reached where the stable solid phase is the metallic state the interaction between the catalytic entity and the oxygen-rich graphite substrate is weakened and particles are reformed at edge regions and then proceed to cut channels across the graphite basal plane. This modification in catalytic action is found in several other systems where oxide to metal transformations are known to occur (*13*).

This type of *in situ* electron microscopy experiment highlights the tremendous advantages of being able to directly observe and obtain the detailed kinetics of subtle changes in the reactivity of the catalyst. These particular aspects would be impossible to ascertain based on data acquired either from a postreaction electron microscopy examination or from macroscale kinetics studies (i.e., thermogravimetric analysis). If we compare the values obtained for the apparent activation energies in the present study with those reported from bulk experiments of 49.4 (*3*) and 30 kcal/mole (*14*) there are certain discrepancies. However, when one takes into consideration the complexity of the rate data presented in Fig. 2, it becomes clear that a bulk experiment would not discriminate between the reactive states of the catalyst and as a consequence the activation energy derived from such an experiment would depend on the temperature range over which measurements were made.

Based on the information derived from the *in situ* electron microscopy experiments it should be possible to select the conditions for either a maximum or a minimum gasification rate in the cobalt/graphite–oxygen reaction. For example, at a temperature of about 650°C, one has the option of having either a high or a relatively low rate of reaction (a difference of two orders of magnitude) depending on the oxidation state of the catalyst. We believe that the reactivity of the system can be manipulated by careful choice of the pretreatment conditions (i.e., preheating in an inert gas to a temperature at which a desired state is formed and then introducing oxygen at this stage). This finding is extremely important to the successful operation of processes requiring either acceleration or inhibition of carbon oxidation.

It is interesting to compare the behavior of cobalt with nickel and iron for the graphite–oxygen reaction. Very little catalytic action was observed during *in situ* electron microscopy studies of the interaction of nickel (*8*) and iron (*9*) with graphite. While these additives remained in a low oxidation state there was some evidence for the formation of short channels and pits on the graphite surface; however, as the reaction proceeded the particles were converted to the highest oxidation states and this aspect coin-

cided with the complete suppression of catalytic activity. This situation can be best understood from a consideration of the thermodynamic calculations of the possible transitions which can occur in these three systems. We believe that the high catalytic activity of cobalt is attributable to its ability to readily undergo redox cycles at all temperatures, a necessary requirement of the oxygen-transfer mechanism which accounts for catalytic oxidation of graphite (*2, 15, 16*). In contrast, nickel and iron tend to form very stable oxides in the presence of oxygen, which are not easily reduced by carbon and as a consequence the particles cannot perform the redox cycle and these additives do not exhibit any significant catalytic activity for the graphite–oxygen reaction.

(*b*) *Cobalt/Graphite–Hydrogen*

Although wetting and spreading of metal particles at graphite edges during the early stages of reaction in hydrogen appear to be general phenomena, for most single metals the subsequent catalytic attack by edge recession is limited to a narrow temperature range. In the case of cobalt, however, this form of attack is more extensive, taking place from 450 to 650°C. This result is not entirely unexpected, in view of the work of Weisweiler and Mahadevan (*17*), who reported that the interfacial energy of cobalt with graphite is considerably lower than that of either nickel or iron with the same material. As a consequence cobalt will exhibit a stronger interaction with the carbon edge atoms than either of the other metals and tend to accelerate the gasification process by the edge recession mode. Recent studies have shown that careful control of this type of interaction can have a profound effect on the catalyst particle dispersion characteristics (*18*).

The gradual decrease in the rate of edge recession and the concomitant reappearance of discrete particles is also a common occurrence in many metal/graphite–hydrogen systems. The reasons for the transition in particle morphology and the consequent change in mode of catalytic action from edge recession to channeling are related to a modification in wetting characteristics between the metal and the graphite. It has been reported by a number of workers (*19–21*) that when a critical amount of carbon is dissolved in such metals as iron, cobalt, and nickel, then an abrupt change from wetting to nonwetting takes place at the metal graphite interface. Based on this information it is tempting to rationalize the morphological changes observed in metal/graphite–hydrogen systems with an increase in the concentration of dissolved carbon in the particles at high temperatures.

A comparison of the intrinsic channeling rates of iron, cobalt, and nickel on the graphite–hydrogen reaction is presented in Fig. 6. To allow for the effects of particle size and channel depth on rate, the data used to construct these plots were normalized to 25-nm-diameter particles cutting channels of similar depth. At 900°C it is clear that cobalt is significantly more active than either nickel or iron. This finding is consistent with the data reported by McKee (*22*) from bulk studies, but is in disagreement with the conclusions reached by Tomita and Tamai (*4*), who found that nickel was the most active of these three metals. The results of this latter study, however, should be treated with caution since these workers elected to use metal chlorides as the catalyst precusor, and therefore the graphite was probably contaminated with strongly adsorbed halide ions. The consequences of exposing a specimen to a chlorine environment prior to performing a catalytic hydrogasification of graphite experiment were highlighted by Baker and co-workers (*23*). Using the *in situ* electron microscopy technique they observed that when a small amount of chlorine was added to the hydrogen feedstream the channeling action of platinum particles across the graphite basal plane ceased, and this condition persisted even when the halogen was removed from the system. It was necessary to carry out an intermediate oxidation step in order to restore catalytic at-

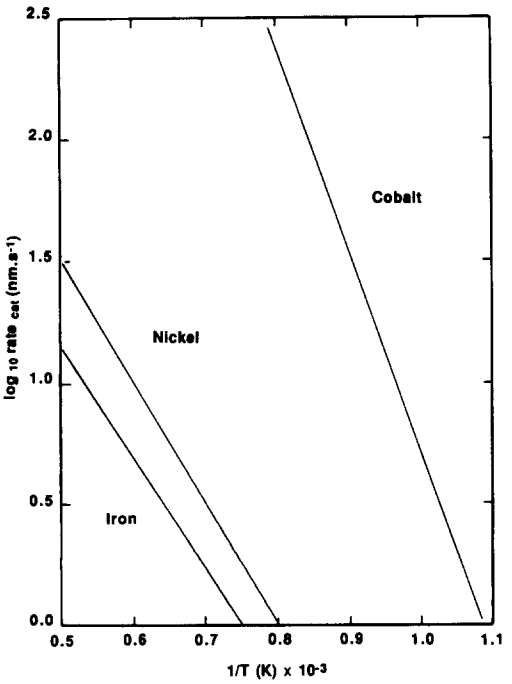

FIG. 6. Comparison of the catalytic effect of iron, nickel, and cobalt on the graphite–hydrogen reaction.

tack of the deactivated specimen. Clearly, contact of a graphite specimen with a halogen-containing molecule should be avoided if meaningful gasification rates are to be obtained.

Finally, it is interesting to find that cobalt does not appear to exhibit the same tendency as iron and nickel to deactivate at temperatures of around 1000°C. Deactivation of metals in the graphite–hydrogen reaction has been attributed to the accumulation of graphitic overlayers on the catalyst particle surfaces (*9*). This condition occurs when the rate of carbon formation becomes faster than the rate of removal by hydrogen species to form methane. Eventually total encapsulation of the particle surface takes place and the gasification reaction ceases. In the case of cobalt it is probable that the rate of hydrogasification is sufficiently high so that carbon does not have a chance to build up on the particle surfaces at the conditions where the present experiments were performed.

SUMMARY

The results of this investigation show that cobalt exhibits a significantly higher catalytic activity for the gasification of graphite in oxygen and hydrogen than either iron or nickel. The complex pattern of behavior found for the cobalt/graphite–oxygen system has been resolved by direct observation of the interfacial behavior and the intrinsic kinetic behavior of the catalyst at various stages of the reaction and the supporting evidence obtained from the use of the powerful new technique of *in situ* electron diffraction. From these measurements it was found that in the initial stages of the reaction CoO was the catalytic entity, which gradually converted to Co_3O_4 as the temperature was raised. Both these oxides increase the rate of gasification by the edge recession mode due to the strong interaction with oxygenated graphite surface. At the highest temperatures a dramatic change in the wetting characteristics of the catalyst on the graphite was observed indicating a weakening of the interaction between the two components. This transformation can be related to the existence of metallic cobalt and is consistent with a change in catalytic action from edge recession to channeling.

It is suggested that the ability of cobalt to maintain its catalytic activity in the graphite–hydrogen reaction up to high temperatures is related to the faster rate of removal of carbon from the catalyst surface compared to that of carbon accumulation at these sites.

APPENDIX

Estimation of d-Spacing Change Using Thermal Linear Expansion Data

At temperature T,

$$R_G d_{G'} = R_M d_{M'}$$

$$d_{G'} = d_G(1 + \alpha_G)$$

$$d_{M'} = d_M(1 + \alpha_M),$$

where

$\alpha = \Delta L/L_0$ is percentage of thermal linear expansion (calculated from equations given in Ref. (*24*);

R_G and R_M are the measured distances from the diffraction patterns for graphite and the unknown compound, respectively;

d_G and d_M are d-spacings for graphite and the unknown compound at room T;

$d_{G'}$ and $d_{M'}$ are d-spacings for graphite and the unknown compound at a given reaction T.

Then,

$$R_G d_G (1 + \alpha_G) = R_M d_M (1 + \alpha_M).$$

Therefore,

$$d_M = R_G d_G / R_M \times (1 + \alpha_G)/(1 + \alpha_M).$$

If,

$$C = (1 + \alpha_G)/(1 + \alpha_M)$$

then,

$$d_M = C \times R_G d_G / R_M.$$

Based on experimental linear thermal expansion data (*24*) the values of C (correction factor) for two temperatures 500 and 1000°C were calculated and are expressed relative to graphite in Table 5. Unfortunately, experimental lattice parameter data as a function of temperature for the compounds of interest in the current work are limited and the only information which exists is for cobalt (*25*). From Table 5 it can be seen that the correction factor, C, for cobalt calculated from α values is in close agreement with that obtained from calculations using the lattice parameter data reported by Nishizawa and Ishida (*25*). In the absence of relevant experimental data we feel that the theoretical treatment adopted in this work provides a viable approach to account for the variations in the lattice parameter values resulting from an increase in temperature.

TABLE 5

Correction for Changes in d-Spacings as a Function of Temperature

Compound	% Thermal expansion (α)		Correction factor (C)	
	500°C	1000°C	500°C	1000°C
Graphite	0.37	0.79	1.0	1.0
Co[a]	0.65	1.46	0.997	0.993
Co[b]	0.63	1.28	0.997	0.995
CoO	0.62	1.33	0.998	0.995
Co_3O_4	Not available	Not available	—	—

[a] Based on linear thermal expansion data (Ref. (*24*)).

[b] From lattice parameter data (Ref. (*25*)).

ACKNOWLEDGMENTS

The authors are indebted to Dr. N. M. Rodríguez, who performed the *in situ* electron diffraction examinations. Financial support for this research was provided by the United States Department of Energy, Basic Energy Sciences, Grant DE-FG05-89ER14076.

REFERENCES

1. Thomas, J. M., and Walker, P. L., Jr., *Carbon* **2,** 163 (1964).
2. McKee, D. W., *Carbon* **8,** 623 (1970).
3. Heintz, E. A., and Parker, W. E., *Carbon* **4,** 473 (1966).
4. Tomita, A., and Tamai, Y., *J. Catal.* **27,** 293 (1972).
5. Tomita, A., and Tamai, Y., *J. Phys. Chem.* **78,** 2254 (1974).
6. Tamai, Y., Watanabe, H., and Tomita, A., *Carbon* **15,** 103 (1977).
7. Keep, C. W., Terry, S., and Wells, M., *J. Catal.* **66,** 451 (1980).
8. Baker, R. T. K., and Sherwood, R. D., *J. Catal.* **70,** 198 (1981).
9. Baker, R. T. K., Chludzinski, J. J., and Sherwood, R. D., *Carbon* **23,** 245 (1985).
10. Baker, R. T. K., and Harris, P. S., *J. Phys. E.* **5,** 793 (1972).
11. Rodriguez, N. M., Oh, S. G., Downs, W. B., Pattabiraman, P., and Baker, R. T. K., *Rev. Sci. Instrum.* **61,** 1863 (1990).
12. Goethel, P. J., and Yang, R. T., *J. Catal.* **101,** 342 (1986).
13. Baker, R. T. K., *Carbon* **24,** 715 (1986).
14. Surski, G. A., Emel'yanova, V. M., Denisovkaya, I. E., Avdeenko, M. A., and Vasiliev, Yu. N., *Izv. Akad. Nauk SSR Neorg. Mater.* **23,** 1847 (1987).
15. Neumann, B., Kroger, C., and Fingas, E., *Z. Anorg. Chem.* **197,** 321 (1931).
16. Amariglio, H., and Duval, X., *Carbon* **4,** 323 (1966).
17. Weisweiler, W., and Mahadevan, V., *High Temp.-High Pressures* **4,** 27 (1972).

18. Chang, T. S., Rodriguez, N. M., and Baker, R. T. K., *J. Catal.* **123,** 486 (1990).

19. Naidich, Yu. V., and Kołesnichenko, G. A., *Parosh Met.* **6,** 55 (1961).

20. Humenik, M., Hall, D. W., and van Alsten, R. L., *Metal Progr.* **4,** 101 (1962).

21. Naidich, Yu. V., Petevertailo, V. M., and Nevodnik, G. M., *Parosh. Met.* **11,** 58 (1971).

22. McKee, D. W., *Carbon* **12,** 453 (1974).

23. Baker, R. T. K., Lund, C. R. F., and Dumesic, J. A., *Carbon* **21,** 469 (1983).

24. Touloukian, Y. S., Kirby, R. K., Taylor, R. E., and Lee, T. Y. R., *in* "Thermophysical Properties of Matter," Vols. 12 and 13. IFI/Plenum, New York, 1977.

25. Nishizawa, T., and Ishida, K., *Bull. Alloy Phase Diagrams* **4,** 388 (1983).